

# Photocatalytic degradation of DNOC in aqueous TiO<sub>2</sub> dispersions Investigation of the initial reaction steps

D. Fabbri<sup>a</sup>, L.S. Villata<sup>b</sup>, A. Bianco Prevot<sup>a</sup>, A.L. Capparelli<sup>b</sup>, E. Pramauro<sup>a,\*</sup>

<sup>a</sup> Dipartimento di Chimica Analitica, Università di Torino, Via P. Giuria 5, 10125 Turin, Italy

<sup>b</sup> INIFTA, Departamento de Química, Facultad de Ciencias Exactas, Universidad de La Plata-CONICET,  
Casilla de Correo 16, Sucursal 4, 1900 La Plata, Argentina

Received 28 July 2005; received in revised form 6 October 2005; accepted 11 October 2005

Available online 16 November 2005

## Abstract

The photocatalytic transformation of the pesticide 4,6-dinitro-*o*-cresol (DNOC) over irradiated TiO<sub>2</sub> suspensions was investigated in aerated aqueous solutions. Complete and relatively fast substrate degradation was achieved after irradiation with simulated solar light, being the reaction rate dependent on the initial pH. The slower evolution of the mineralization process, which can be accomplished after longer irradiation times, was evidenced by monitoring the dissolved organic carbon decrease and the formation of nitrogen inorganic products.

Both the analysis of the reaction end-products and the HPLC–MS characterization of the organic intermediates are consistent with a reaction mechanism where the hydroxylation of the aromatic ring and the oxidation of the methyl group can play a major role as initial reaction steps and occur at comparable rates. The direct reduction of nitro groups at the semiconductor surface to form ammonium ion, inferred from the MS analysis of minor aromatic intermediates, appears to be another viable reaction path.

The nearly quantitative mineralization of the pesticide has been observed after long term (3 h) irradiation, time after which no aromatic products were detected.

© 2005 Elsevier B.V. All rights reserved.

**Keywords:** Photocatalysis; DNOC; Intermediates; Degradation mechanism

## 1. Introduction

For several decades in the past century, 4,6-dinitro-*o*-cresol (DNOC) has been used worldwide, largely as herbicide against broadleaf annual weeds in many crops, but also as insecticide, fungicide and even as additive in some dietary products. Despite DNOC was banned as pesticide from EC and USA about 15 years ago, it is still employed in some developing countries and relevant stocks of this product are present in Eastern Europe, where the problem of DNOC disposal and destruction has been recently considered [1].

Due to its relatively low  $pK_a$  value (around 4.3 [2]) DNOC is usually present in its anionic form in aquifers and negligible adsorption is expected in aqueous streams containing very low amounts of suspended organic matter.

The removal of DNOC from aqueous media can be performed using different techniques including biological treatments, physical phase-transfer methods or application of destructive techniques leading to the decomposition of the pollutant molecule. Heterogeneous photocatalysis, a very promising advanced oxidation process (AOP) developed in the past years, allows to perform the efficient degradation and in most cases the complete mineralization of a great variety of organic pollutants present at low concentration levels in aqueous wastes [3–9]. It is based on the use of proper semiconductor materials, which upon activation with suitable light sources give rise to the formation of various reactive species.

The fundamentals of photocatalysis, abundantly described in the literature, can be summarised as follows: irradiation with light of wavelength of energy higher than the band-gap causes electron excitation from the semiconductor valence band to the conduction band, generating electron–holes pairs. Both electrons and holes migrate to the surface of the semiconductor particles, where they can react with water, dissolved oxygen and

\* Corresponding author. Tel.: +39 011 6707631; fax: +39 011 6707615.  
E-mail address: [edmondo.pramauro@unito.it](mailto:edmondo.pramauro@unito.it) (E. Pramauro).

surface OH groups to form various oxidising species, including the highly reactive hydroxyl radicals, whereas superoxide and perhydroxyl radicals are formed from the reaction of excited electrons with oxygen. The reactive oxygen-containing species can attack and oxidise the organic molecules, generally leading to a complete mineralization of the substrate.

To our knowledge, no studies on photocatalytic degradation of DNOC have been reported in the literature until now, although other molecules having similar structures (in particular nitrophenols [10–15] and cresols [16,17]) have been the subjects of previous investigations.

In the present work, we investigated the photocatalytic degradation of DNOC, present in anionic or in undissociate form in aqueous solutions. The effect of initial pH on the kinetics of DNOC abatement was examined, together with the formation and evolution of the end-products arising from the substrate mineralization. In order to give insight into the mechanism of the crucial initial steps of the reaction, subject often disregarded in most similar studies, particular attention was devoted to the identification of the organic intermediates formed before the aromatic ring opening.

## 2. Experimental

### 2.1. Reagents and materials

DNOC (purity 91.5%; water  $9 \pm 1\%$ , from Dr. Ehrenstorfer, Germany), 3,5-dinitrosalicylic acid 98% (Fluka), 4,6-dinitro-2-methyl-resorcinol and 3,5-dinitrosalicylaldehyde 97% (Aldrich), were used as received.

The photocatalyst was TiO<sub>2</sub> Degussa P-25 (composed of ca. 80% anatase and 20% rutile). Any organic impurity of semiconductor was removed by washing with water and by successive irradiation of the dispersion with simulated solar light for about 12 h. The washed semiconductor was then dried in the oven at 80 °C. The resulting powder was resuspended in water by sonication immediately before use.

Acetonitrile (Lichrosolv, Merck) and acetic acid (Merck) were employed as LC eluents. Na<sub>2</sub>CO<sub>3</sub> and NaHCO<sub>3</sub> solutions (Merck) were used as eluents for the IC measurements. H<sub>2</sub>SO<sub>4</sub> and NaOH (Merck) were used to adjust the pH.

A Milli-Q water purification system (Millipore) provided the water used for all solutions and suspensions.

### 2.2. Degradation experiments

All irradiations were performed in stirred cylindrical closed cells (40 mm i.d. × 25 mm high), made of Pyrex glass on 5 mL of aqueous dispersions, containing 0.1 mM of DNOC and 200 mg L<sup>-1</sup> of TiO<sub>2</sub>. A 1500 W Xenon lamp (Solarbox, CO. FO. MEGRA, Milan, Italy) equipped with a 340 nm cut-off filter was employed. The measured photonic flux of the simulated AM1 radiation was ca.  $1.4 \times 10^{-5}$  einstein min<sup>-1</sup> [18]. The temperature within the cells was ca. 55 °C.

The samples were filtered through a cellulose acetate membrane (HA 0.45 μm, Millipore) before the analysis.

### 2.3. Analytical procedures

The substrate degradation was followed by HPLC, employing a Merck-Hitachi instrument, equipped with a L-6200 pump and UV-vis L-4200 detector. A column RP-C18 (Lichrospher, 4 mm i.d. × 125 mm long, from Merck) was used. The eluent was acetonitrile/aqueous solution with 1% of acid acetic 50/50% (v/v), flow rate 1.0 mL min<sup>-1</sup>. The detector wavelength chosen was 269 nm.

The formation of ionic products was followed by a suppressed ion chromatography, employing a Dionex DX 500 instrument equipped with a conductimeter detector (ED 40, Dionex). The anions (nitrate and nitrite) have been analysed by using an AS9HC anionic column (200 mm long × 4 mm i.d.) and an aqueous solution of K<sub>2</sub>CO<sub>3</sub> (10 mM) and NaHCO<sub>3</sub> (4 mM); the elutions were performed at 30 °C, at a flow rate of 1 mL min<sup>-1</sup>. The determination of ammonium ions was performed by employing a CS12A column, using metansulphonic acid 25 mM as eluent at a flow rate of 1 mL min<sup>-1</sup>. Samples having an initial pH 8.0 were acidified with H<sub>2</sub>SO<sub>4</sub> before being analysed.

The evolution of the dissolved organic carbon (DOC) during the photocatalytic runs was followed using a Shimadzu 5000 TOC analyzer (catalytic oxidation on Pt at 680 °C). Calibration was achieved by injection of known amounts of potassium phthalate.

The analysis of intermediates were performed on 20 mL samples, filtered and concentrated to ca. 1 mL by means of evaporation under vacuum at low temperature. A ThermoFinnigan Surveyor MSQ instrument, equipped with a photodiode array detector, an ESI interface and a single quadrupole analyser was used. Two different elution conditions were employed:

- (1) Solvent A was an aqueous solution of acetic acid 1% (w/v) and solvent B was CH<sub>3</sub>CN; a linear gradient was run as follows (*t*, elution time in minutes): *t* = 0, A = 50%, B = 50%; *t* = 10, A = 50%, B = 50%; *t* = 15, B = 100%; *t* = 30 B = 100%. The MS operational parameters were: spray voltage 2.5 kV, temperature of the heated capillary 550 °C and cone voltage 70 V.
- (2) Solvent A was an aqueous solution of triethylamine 0.1% (w/v) and solvent B was CH<sub>3</sub>CN; a linear gradient was applied as follows: *t* = 0, A = 98%, B = 2%; *t* = 10 A = 98%, B = 2%; *t* = 20, B = 100%; *t* = 30, B = 100%. The MS operational parameters were: spray voltage 1.0 kV, temperature of the heated capillary 400 °C and cone voltage 70 V.

The mass spectrometer was operated in the negative scan mode; mass number (*m/z*) range: 50–400.

All LC elutions were carried out using a Lichrospher Merck RP 18 column (250.0 mm × 4.6 mm i.d., dp = 5 mm); mobile phase flow rate: 0.5 mL min<sup>-1</sup>.

## 3. Results and discussion

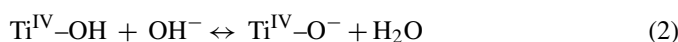
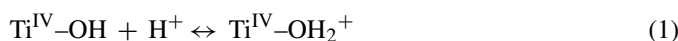
### 3.1. Analysis of the primary process

Before to start with the photocatalytic runs some blank experiments on DNOC were performed in the dark, in the absence

of TiO<sub>2</sub>. No appreciable degradation of the examined compound was observed, thus confirming its photostability under the described irradiation conditions.

The possible adsorption of DNOC on TiO<sub>2</sub> was also investigated, via spectrophotometric analysis, on filtered suspensions prepared at the three examined pH and kept in the dark. The observed DNOC loss was <1% of the initial concentration in all the cases.

The photocatalytic degradation was investigated at different initial pH values: 3.0, 5.4 and 8.0; these conditions were chosen in order to consider different possible interactions between the substrate and the active semiconductor particles. Taking into account that the measured isoelectric point of the employed TiO<sub>2</sub> is around pH 5.6 [16], protonation or deprotonation of surface hydroxy groups takes place at pH values below or above this pH value, respectively, thus introducing a neat electric charge on the semiconductor particles, as shown below:



At pH 3.0 the semiconductor particles are positively charged and the substrate is present in its undissociated form, whereas at pH 5.4 and 8.0 DNOC is mainly present in its anionic form, being the charge of TiO<sub>2</sub> particles nearly zero and negative, respectively. This implies that attractive electrostatic interactions between the substrate molecules and the semiconductor particles should be neglected under the examined experimental conditions.

Fig. 1 shows the evolution of the primary process at the three investigated initial pH values. The DNOC degradation follows a pseudo-first order kinetic law, according to the equation:

$$-\frac{dC_{\text{sub}}}{dt} = k_{\text{obs}} C_{\text{sub}} \quad (3)$$

where  $C_{\text{sub}}$  is the substrate concentration and  $k_{\text{obs}}$  is the observed first-order rate constant. According to Eq. (3), linear plots of  $\ln(C/C_0)$  versus time have been obtained up to ca. 60–80% DNOC degradation (see inset in Fig. 1).

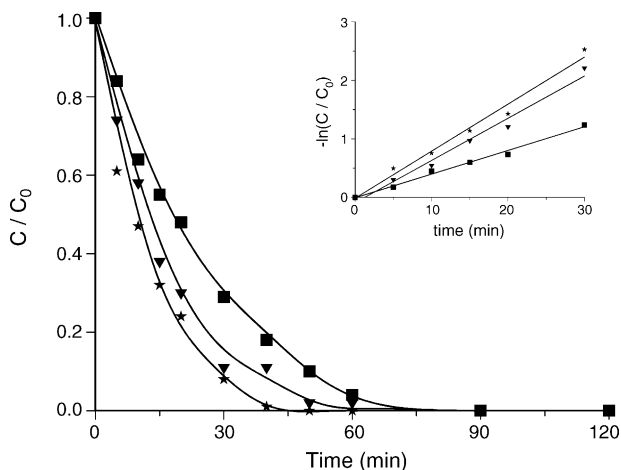
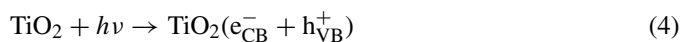


Fig. 1. Photocatalytic degradation of DNOC at pH 3 (■), pH 5.4 (▼) and pH 8 (★). Substrate concentration  $1 \times 10^{-4}$  M, TiO<sub>2</sub> 200 mg L<sup>-1</sup>.

The analysis of the primary process reveals a progressive increase of the degradation rate with increasing initial pH,  $k_{\text{obs}} = 4.0 \times 10^{-2} \text{ min}^{-1}$  (pH 3.0),  $7.2 \times 10^{-2} \text{ min}^{-1}$  (pH 5.4),  $8.0 \times 10^{-2} \text{ min}^{-1}$  (pH 8.0). Complete disappearance of substrate was observed after ca. 90 min irradiation at pH 3.0, after ca. 60 min at pH 5.4, and after ca. 45 min at pH 8.0. The observed pH decrease during the DNOC degradation was very low (<0.2 pH units) in experiments performed at initial pH 3.0 and 5.4, whereas a more significant change has been observed during the runs performed at initial pH 8.0. In fact, the pH measured after 20 min irradiation (time at which about 80% of DNOC has been degraded) was around 7 under these later conditions.

From the above pH data, the absence of attractive interactions between DNOC and TiO<sub>2</sub> during the primary process can be still invoked. After long term irradiation (180 min) the measured final pH was ca. the same found after DNOC degradation for runs performed at pH 3 and 5.4, and around 6 for experiments performed at initial pH 8.

In addition to its expected major role on substrate adsorption, the pH can also influence the occurring electron transfer processes [19] and the formation of crucial oxidizing species. If the formation of reactive  $\bullet\text{OH}$  is considered, the major source of such reactive species are reactions (5) and (6), which are favoured at higher pH values.



However,  $\bullet\text{OH}$  can also be generated starting from a series of reactions involving the superoxide radical, mainly formed in reaction (8):



This radical gives rise to the formation of H<sub>2</sub>O<sub>2</sub>, which in turn can originate  $\bullet\text{OH}$  through a well known sequence of reactions [6,7,14]. Although at working pHs lower than ca. 4.9 (value corresponding to the pK<sub>a</sub> of  $\bullet\text{HO}_2$ ) this route of  $\bullet\text{OH}$  formation becomes more significant [15] the role of these reactions has been considered less important than those of processes (5) and (6) [20].

The observed increase of DNOC degradation rate with increasing pH can be justified taking into account that the unfavourable repulsive effects between negatively charged TiO<sub>2</sub> particles and the anionic form of the pesticide (remarkable at pH 8.0 and anyway present at pH values higher than the isoelectric point) can be effectively compensated by the increased formation of  $\bullet\text{OH}$  under these conditions. This behaviour is in good agreement with previous investigations on photocatalytic degradation of 2-nitrophenol [12] and 2,6-dinitrophenol [15], for which the increase of reaction rate with increasing pH was reported in the same pH range (3–8) here examined.

Table 1  
Formation of nitrogen-containing products

pH	<i>t</i> (min)	NO <sub>2</sub> <sup>-</sup> (%)	NO <sub>3</sub> <sup>-</sup> (%)	NH <sub>4</sub> <sup>+</sup> (%)	N <sub>tot</sub> (%)
3	90	2	63	17	82
	180	–	74	23	97
5.4	60	1	59	11	71
	180	–	81	12	93
8	50	3	30	5	38
	180	–	97	5	102

### 3.2. Evolution of substrate mineralization

#### 3.2.1. Formation of nitrogen-containing products

It is well known from the literature [21,22] that the photocatalytic degradation of aromatic molecules containing nitro groups, like nitrophenols, leads to the formation of nitrate and ammonium ions as main nitrogen mineralization products. The presence of nitrite as transient intermediate, also detected in these experiments, has been explained admitting that  $\bullet\text{OH}$  attack can lead to the replacement of nitro groups (considered as good leaving groups) by OH in these molecules [23].

Table 1 reports the percentage of nitrite, nitrate, ammonium and total nitrogen released at times corresponding to the complete disappearance of DNOC and after long term irradiation (180 min).

Nitrite concentration increases until a maximum value, but decreases rapidly and vanishes with subsequent irradiation due to further oxidation of this product to NO<sub>3</sub><sup>-</sup> by  $\bullet\text{HO}$  [24]. At pH 3.0 and 5.4 the maximum percentage of nitrite (ca. 6–7% of the stoichiometric nitrogen) is produced after ca. 15 min of irradiation, whereas at pH 8.0 the same percentage is reached after longer irradiation times (ca. 40 min).

As far as the formation of NO<sub>3</sub><sup>-</sup> and NH<sub>4</sub><sup>+</sup> is concerned, we observed a continuous increase of NO<sub>3</sub><sup>-</sup> formation by increasing the irradiation time. This product represents about 80% of total nitrogen after 180 min irradiation at pH 5.4, value in good agreement with previous findings reported for 2,4-dinitrophenol under similar conditions [25]. Upon increasing the irradiation time the ammonium to nitrate ratio becomes lower due to a slow oxidation of NH<sub>4</sub><sup>+</sup>. For DNOC, the measured NH<sub>4</sub><sup>+</sup>/NO<sub>3</sub><sup>-</sup> ratio after 180 min irradiation at pH 5.4 (0.15) is near to that reported for 2,4-dinitrophenol [22].

If the release of total inorganic nitrogen is considered (see Fig. 2), the corresponding rates are in the order pH 3.0 > pH 5.4 > pH 8.0 when short irradiation times (ca. 30 min) are considered. For longer irradiation times (40–90 min) a neat decrease of the rate of total nitrogen formation is observed in experiments performed at pH 3.0 and 5.4, whereas the formation of nitrogen products proceeds at a nearly constant rate at pH 8.0. The stoichiometric mineralization of nitrogen was achieved after ca. 120 min at pH 8.0, whereas at this time the formation of nitrogen end-products is still incomplete at pH 3.0 and 5.4.

The perusal of Fig. 2 shows that the release of inorganic nitrogen occurs at a lower rate in respect to the primary process; in fact the percent of total nitrogen not transformed into min-

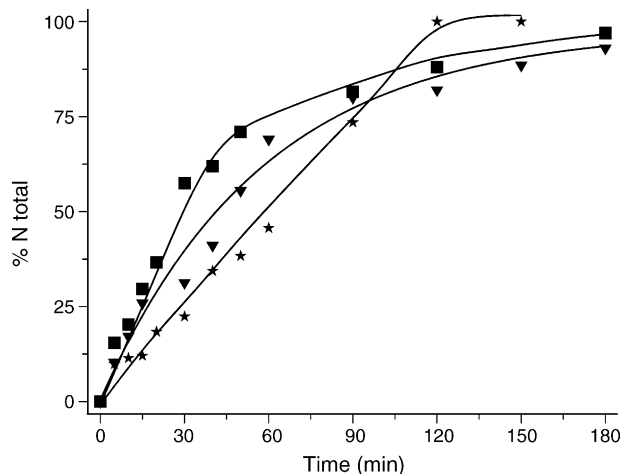


Fig. 2. Evolution of total percentage of nitrogen released as NO<sub>3</sub><sup>-</sup>, NO<sub>2</sub><sup>-</sup> and NH<sub>4</sub><sup>+</sup> during the DNOC degradation at pH 3 (■), pH 5.4 (▼) and pH 8 (★). Substrate concentration  $1 \times 10^{-4}$  M, TiO<sub>2</sub> 200 mg L<sup>-1</sup>.

eralization products after the complete abatement of DNOC is significant (ca. 60% at pH 8.0, ca. 30% at pH 5.4, ca. 20% at pH 3.0) and this implies the existence of reaction intermediates still containing nitrogen. Taking into account that no traces of aromatic compounds were detected at the end of the primary process, the residual organic nitrogen must be associated with the presence of organics coming from the ring opening.

Anyway, the nitrogen mass-balance at longer irradiation times confirms (within the uncertainties of the analytical methods employed) the almost stoichiometric mineralization of this component, also taking into account that the formation of low amounts of gaseous products such as N<sub>2</sub> or nitrogen oxides during the photocatalytic oxidation of ammonia cannot be completely excluded [26].

#### 3.2.2. DOC evolution

Fig. 3 shows the decrease of dissolved organic carbon during the treatment at the three initial pHs considered. A slight residual concentration of DOC (ca. 6% of the initial content) was found

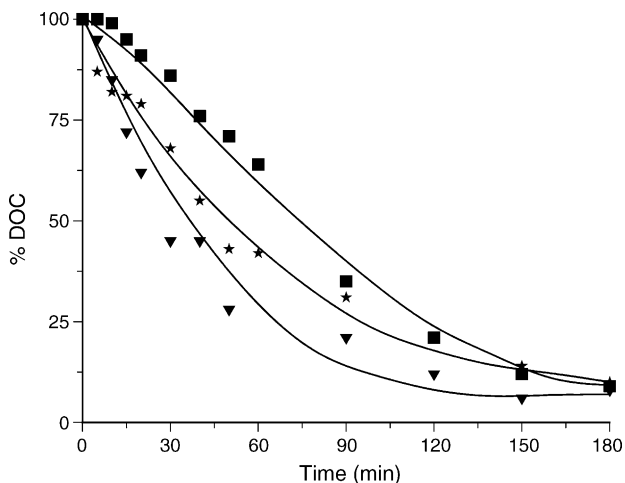


Fig. 3. Evolution of DOC during the DNOC degradation at pH 3 (■), pH 5.4 (▼) and pH 8 (★). Substrate concentration  $1 \times 10^{-4}$  M, TiO<sub>2</sub> 200 mg L<sup>-1</sup>.

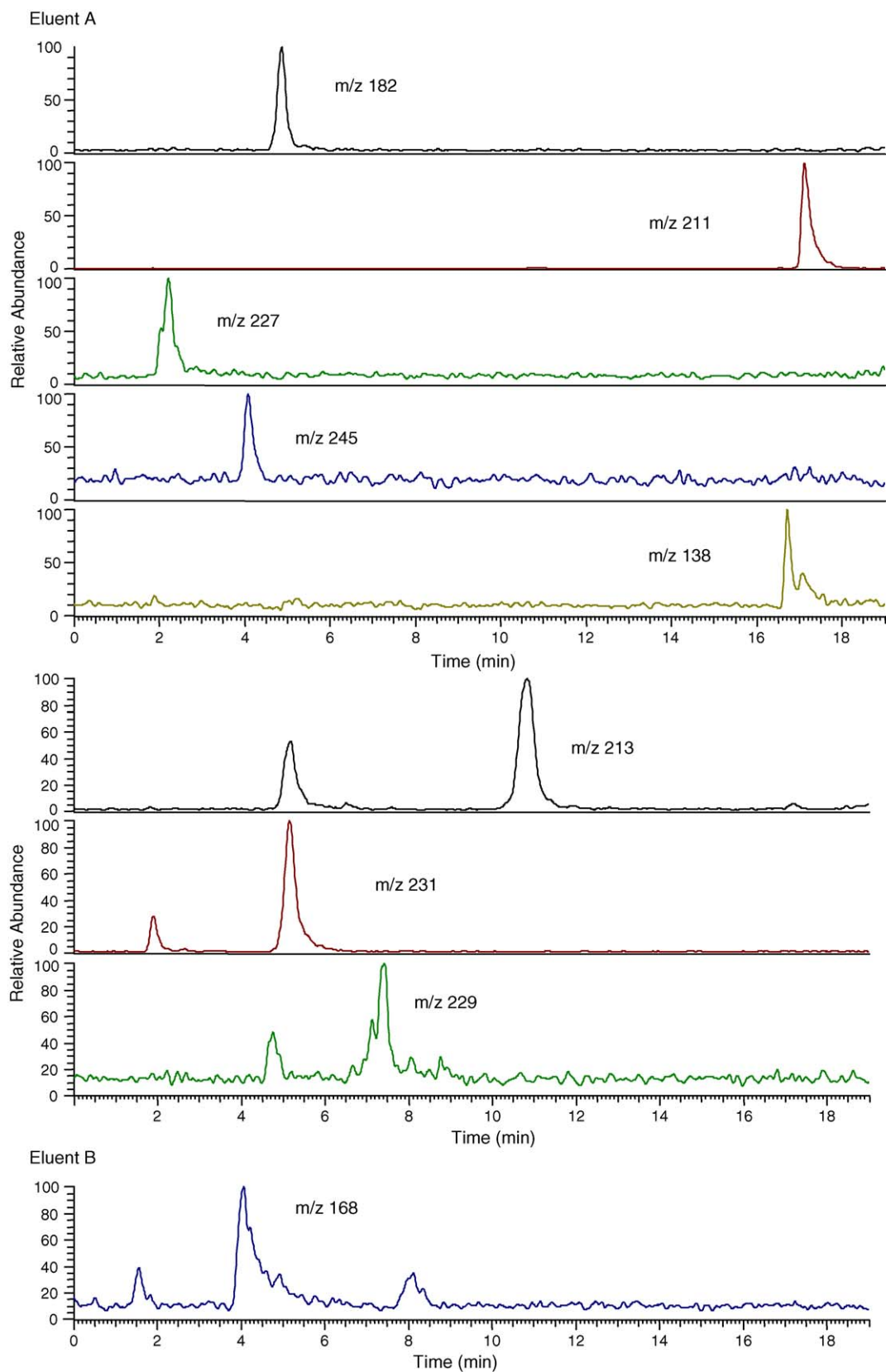


Fig. 4. Chromatographic profiles of the solution after 5 min irradiation showing the intermediate species formed from DNOC degradation at pH 5.4; ion extracted from full scan chromatogram. Eluent A: triethylamine and acetonitrile; eluent B: acetic acid and acetonitrile.

even after 180 min irradiation, indicating a slow mineralization process. The mineralization is anyway faster at pH 5.4.

Also here the observed incomplete DOC elimination after the DNOC abatement (the measured residual DOC is ca. 30, 40 and 50% at pHs 5.4, 8.0 and 3.0, respectively) can be attributed to the presence of residual organic compounds, which are in turn degraded more slowly.

### 3.3. Formation of reaction intermediates

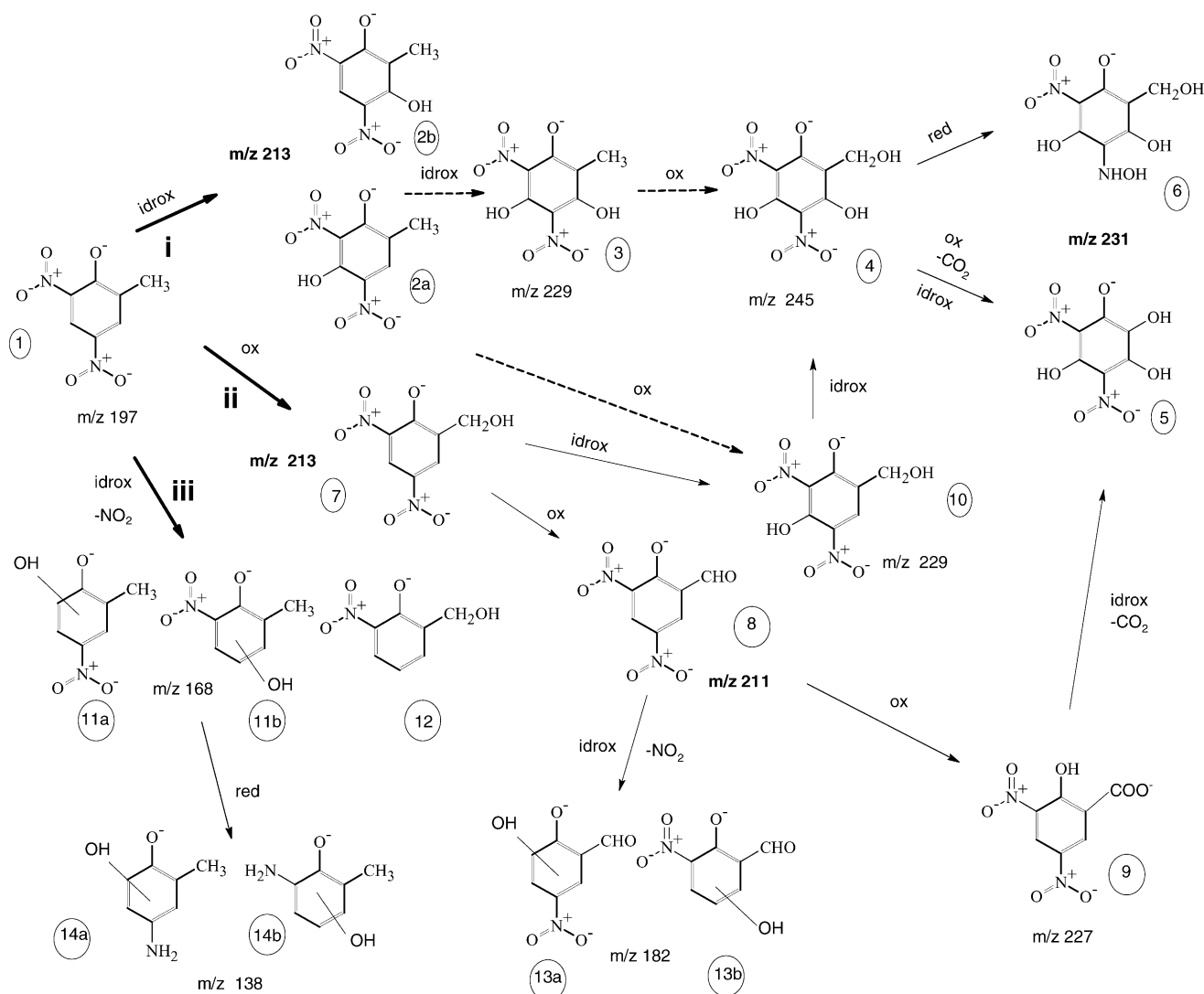
The appearance and evolution of some transient chromatographic peaks has been observed during the HPLC monitoring of the primary process. The investigation of the nature of these intermediates was performed via HPLC–DAD–MS analysis on solutions irradiated at the three pHs values examined. Samples were taken after 5 and 10 min irradiation, times at which the aromatic intermediates are better evidenced. No aromatic products were detected, within the sensitivity limits of the employed techniques, after irradiation times corresponding to the complete degradation of DNOC.

Fig. 4 shows different digital reconstructions, at various significant  $m/z$  values, of the chromatographic pattern of the sample degraded at pH 5.4. Since also the solutions treated at pHs 3 and 8 showed similar profiles, these observations support the hypothesis that pH mainly affects the DNOC abatement kinetics, whereas the degradation mechanism remains essentially the same.

The MS analysis showed the presence of three main peaks, corresponding to the more abundant intermediates having 231, 213 and 211  $m/z$ , and a certain number of minor peaks. The intermediates structures have been proposed on the basis of the evidenced  $m/z$  values and considering the corresponding MS spectra fragmentation.

Scheme 1 shows a possible reaction mechanism involving different paths (the dashed lines indicate the less probable reactions) taking into account that, due to the specific characteristics of the LC–MS technique, the univocal identification of all the present species is not a simple task.

It can be noticed that all the described intermediates are aromatic in nature, as confirmed by the diode-array analysis of



Scheme 1.

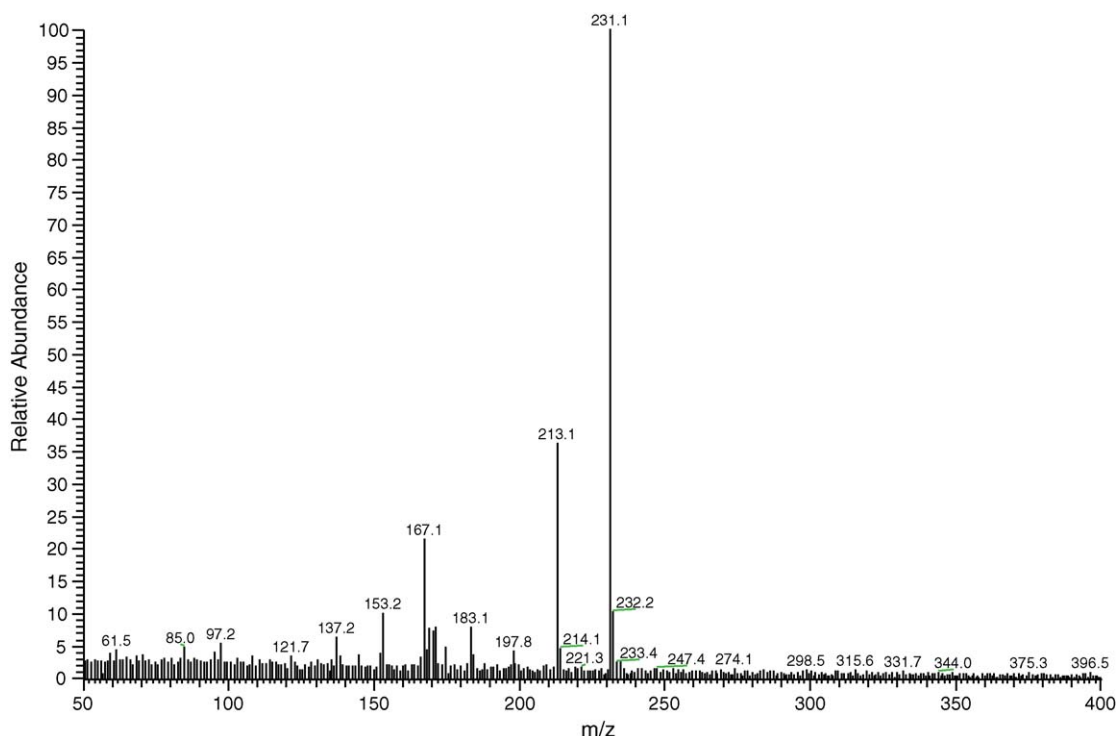


Fig. 5. MS spectrum of the peak attributed to structure (5).

the corresponding peaks, and most of them are consistent with structures still keeping one or two nitro groups. The chromatographic retention times of some of the observed peaks ( $m/z$  231 and 245) are consistent with the behaviour of compounds more hydrophilic than DNOC, as expected if the hydroxylation of the aromatic ring (largely supported by the literature data) takes place.

If the more abundant intermediates are considered, compound (8) corresponding to  $m/z$  211 has been confirmed by means of its authentic standard. Two peaks have been found for compounds having  $m/z$  231, for which the structures (5) and (6) have been hypothesised. Fig. 5 reports the MS spectrum of the peak attributed to structure (5), where the fragments with  $m/z$  213, 167, 183 and 153 can be obtained from the loss of one molecule of water ( $-18$ ), one of  $\text{NO}_2$  ( $-46$ ) and two consecutive  $\text{NO}$  groups ( $-30$  for each group), respectively. On the other hand, no significant information have been obtained from the MS spectrum of the other observed peak, for which structure (6) could be proposed; nevertheless, this structure cannot be completely excluded since it is consistent with the whole degradation scheme.

For the third abundant intermediate, corresponding to  $m/z$  213, only one peak has been detected, but three isomeric structures (2a), (2b) and (7) are possible. Although ring hydroxylation has been reported to be a very important degradation route for various aromatic derivatives, in our case the electron withdrawing nature of nitro groups reduces the electronic density of the ring which becomes less reactive towards the electrophilic attack by  $\bullet\text{OH}$ , but the ortho position in respect to the methyl group is relatively less deactivated in DNOC and hydroxylation in this position could probably occur. However, compound (2b) can be

reasonably excluded because the corresponding authentic standard shows a very different retention time.

Since the presence of two nitro groups favours the oxidation of methyl group in respect to ring hydroxylation, the formation of compound (7) should be more probable. This hypothesis is supported by the identification of compounds (8) and (9), both confirmed through the analysis of the corresponding authentic standards. From compound (9), decarboxylation and hydroxylation processes can lead to the formation of the hypothesised compound (5).

As far as the minor components is concerned, for  $m/z$  229 the analysis of the corresponding MS spectrum did not provide useful information to discriminate between the possible structures (3) and (10), but previous considerations about the facilitated methyl group oxidation lead to suggest compound (10) as the more probable structure.

The above discussed part of the Scheme evidenced therefore two possible degradation pathways: (i) the  $\bullet\text{OH}$  radical attack on the ring to form 5-hydroxy-4,6-dinitro-*o*-cresol (2a) followed by further hydroxylation and oxidation, finally leading to formation of 2,3,5-trihydroxy-4,6-dinitrophenol (5); (ii) the methyl group oxidation to form alcohol (7), then aldehyde (8) and acid (9).

The formation of substrate derivatives still having one or two nitro groups before the break of the aromatic ring, sustained by the above discussed MS data, suggests that the elimination of nitrous acid as leaving group in DNOC is not so easy as mentioned in the case of simpler nitrophenolic molecules [14].

A third degradation path (iii) can lead to the elimination of one nitro group, accompanied by the hydroxylation of the molecule. This pathway, which is in agreement with the observed nitrite formation, lead us to propose the formation of com-

pounds having the possible structures (11a), (11b) and (12); the same sequence of reactions could be reasonably invoked to justify the formation of the hypothesised derivatives (13a) and (13b) starting from the intermediate (8). The degradation path (iii) can further originate compounds (14a) and (14b), having  $m/z$  138, through a reductive step, which is consistent with previous findings sustaining the possible  $e_{CB}^-$  capture by nitroaromatic substrates at the semiconductor/solution interface [27,18].

Since compounds from (11) to (14) were detected at very low concentration levels, they have been discussed in the frame of a general possible mechanism without consider in detail which isomer could be effectively present. It must be noted that for each  $m/z$  ratio corresponding to the observed minor compounds, only a single chromatographic peak has been evidenced, thus supporting the hypothesis that one of the possible isomers largely predominates.

#### 4. Conclusions

The photocatalytic degradation of DNOC is relatively fast (within 50–90 min) in aqueous media under the examined conditions, but the persistence of organic intermediates after the substrate abatement suggests the need for longer treatment times in view of potential environmental applications. The HPLC–MS analysis of the organic compounds formed during the initial steps of the degradation allows to propose a possible reaction mechanism where the hydroxylation of the DNOC aromatic ring and the oxidation of the methyl group, considered as crucial paths during the early events, proceed simultaneously. The examination of the MS spectra of other compounds, found at much lower concentration levels, were consistent with the presence of a possible reduction route through which the transformation of nitro groups of DNOC into  $NH_4^+$  may occur.

At reaction times corresponding to the end of the primary process the abatement of the aromatic transient intermediates was found to be complete, whereas the transformation of residual products coming from the ring opening into the inorganic end-products takes place more slowly. The nature of these compounds, as inferred from the analytical data is basically non-aromatic and then non-toxic. The evolution of inorganic nitrogen and DOC with time allows to estimate in more than 3 h the time necessary to obtain the complete mineralization of the substrate.

#### Acknowledgements

The authors thank Prof. M. Vincenti for helpful discussions about the MS data. Financial support from MIUR (Rome) is gratefully acknowledged by D.F., A.B.-P. and E.P.

L.S.V and A.L.C thank CONICET (Grant PIP 2470/00) and ANPCyT (PICT 06-12610) and UNLP for the financial support.

#### References

- [1] J. Bieganska, *Environ. Sci. Technol.* 39 (2005) 1190–1196.
- [2] M.M. Broholm, N. Tuxen, K. Rugge, P.L. Bjerg, *Environ. Sci. Technol.* 35 (2001) 4789–4797.
- [3] M. Schiavello (Ed.), *Photocatalysis and Environment. Trends and Applications*, Kluwer Academic Publishers, Dordrecht, 1988.
- [4] D.F. Ollis, E. Pelizzetti, N. Serpone, in: N. Serpone, E. Pelizzetti (Eds.), *Photocatalysis. Fundamentals and Applications*, Wiley, New York, 1989, pp. 603–606 (Chapter 18).
- [5] P. Pichat, C. Guillard, C. Maillard, L. Amalric, J.C. D'Oliveira, in: D.F. Ollis, H. Al-Ekabi (Eds.), *Photocatalytic Purification and Treatment of Water and Air*, Elsevier, Amsterdam, 1993, pp. 207–223.
- [6] D. Bahnemann, J. Cunningham, M.A. Fox, E. Pelizzetti, P. Pichat, N. Serpone, in: G.R. Helz, R.G. Zepp, D.G. Crosby (Eds.), *Aquatic and Surface Photochemistry*, Lewis Publications, Boca Raton, FL, 1994, pp. 261–316 (Chapter 21).
- [7] M.R. Hoffmann, S.T. Martin, W. Choi, D.W. Bahnemann, *Chem. Rev.* 95 (1995) 69–96.
- [8] A. Fujishima, T.N. Rao, D.A. Tryk, *J. Photochem. Photobiol. C: Photochem. Rev.* 1 (2000) 1–21.
- [9] S. Malato, J. Blanco, A. Vidal, C. Richter, *Appl. Catal. B: Environ.* 37 (2002) 1–15.
- [10] V. Augugliaro, L. Palmisano, M. Schiavello, A. Sclafani, L. Marchese, G. Martra, F. Miano, *Appl. Catal.* 69 (1991) 323–340.
- [11] M.S. Dieckmann, K.A. Gray, *Water Res.* 5 (1996) 1169–1183.
- [12] K.-H. Wang, Y.-H. Hsieh, M.-Y. Chou, C.-Y. Chang, *Appl. Catal. B: Environ.* 21 (1999) 1–8.
- [13] M. Ksibi, A. Zemzemi, R. Boukchina, *J. Photochem. Photobiol. A: Chem.* 159 (2003) 61–70.
- [14] A. Di Paola, V. Augugliaro, L. Palmisano, G. Pantaleo, E. Savinov, *J. Photochem. Photobiol. A: Chem.* 155 (2003) 207–214.
- [15] B. Swarnalatha, Y. Anjaneyulu, *J. Mol. Catal. A: Chem.* 223 (2004) 161–165.
- [16] R. Terzian, N. Serpone, C. Minero, E. Pelizzetti, *J. Catal.* 128 (1991) 352–365.
- [17] B. Pal, T. Hata, K. Goto, G. Nogami, *J. Mol. Catal. A: Chem.* 169 (2001) 147–155.
- [18] V. Maurino, C. Minero, E. Pelizzetti, P. Piccinini, N. Serpone, H. Hidaka, *J. Photochem. Photobiol. A: Chem.* 109 (1997) 171–176.
- [19] M. Grätzel, *Heterogeneous Photochemical Electron Transfer*, CRC Press, Boca Raton, FL, 1989.
- [20] C. Kormann, D.W. Bahnemann, M.R. Hoffmann, *Environ. Sci. Technol.* 22 (1988) 798–806.
- [21] P. Piccinini, C. Minero, M. Vincenti, E. Pelizzetti, *Catal. Today* 39 (1997) 187–195.
- [22] G.K.C. Low, S.R. McEvoy, R.W. Matthews, *Environ. Sci. Technol.* 25 (1991) 460–467.
- [23] C. Suarez, F. Louys, K. Günther, K. Eiben, *Tetrahedron Lett.* 8 (1970) 575–578.
- [24] Y. Hori, A. Nakatsu, S. Suzuki, *Chem. Lett.* (1985) 1429–1432.
- [25] K. Tanaka, W. Luesaiwong, T. Tanaka, *J. Mol. Catal. A: Chem.* 122 (1997) 67–74.
- [26] H. Mozzanega, J.M. Herrmann, P. Pichat, *J. Phys. Chem.* 83 (1979) 2251–2255.
- [27] P. Piccinini, C. Minero, M. Vincenti, E. Pelizzetti, *J. Chem. Soc., Faraday Trans.* 93 (1997) 1993–2000.